

## SYNTHESIS AND CHARACTERIZATION OF TiN, TiAlN AND TiAlN/Si<sub>3</sub>N<sub>4</sub> CHEMICAL NANOCOMPOSITE

S. Nallusamy<sup>1,\*</sup>, M. Rajaram Narayanan<sup>2</sup> and S. Hariharan<sup>3</sup>

<sup>1,3</sup>Department of Mechanical Engineering, Dr. M G R Educational and Research Institute,  
Chennai-600095, Tamilnadu, India

<sup>2</sup>Department of Mechanical Engineering, Mount Zion College of Engineering,  
Kerala- 689649, India

\*E-mail: ksnallu@gmail.com

---

### ABSTRACT

Nanocomposite coating is a coating with measurements of grain size or individual layers which could be less than 100 nm and it offers enriched durability and performance. The objective of this article is to present the chemical and mechanical characteristics of nano-coated cutting tools. To improve the machinability and tool life, the cutting tool inserts are coated with nanoparticles of nitride coatings using titanium nitride, titanium aluminium nitride and titanium aluminium nitride with silicon nitride. With the advent of nano composites, a coating of thickness in nanometers has become a reality. The nano coatings are carried out through physical vapor deposition process on thin films, get experimentally tested and are coated on cutting tool insert. These TiN, TiAlN and TiAlN/Si<sub>3</sub>N<sub>4</sub> have been adopted due to their better chemical and mechanical properties. Enrichment of hardness is an important criteria and maximum hardness is obtained through multilayer structurization of composites. In this experimental analysis, the various mechanical properties of thin films like hardness, Young's and reduced modulus of thin films were found through a method called nanoindentation, which was carried out on nine different samples of titanium nitride and the results were interpreted.

**Keywords:** Cutting Tool, Chemical Composition, Wear Rate, Nanoindentation, Mechanical Properties

© RASĀYAN. All rights reserved

---

### INTRODUCTION

Nanotechnology becomes one among the paramount growing tools in engineering and scientific regulations. Nanostructured coatings can be categorized as: nanocrystalline, nano multilayer and nanocomposites. Now a day's, the industries that can manufacture the cutting tool are frequently facing the challenge of minimizing the machined parts cost of the machined surface with enhanced quality. These problems normally deal with developing materials for a cutting tool, superior coating, geometry and surface uniqueness of the cutting tools and effective machining parameters.<sup>1-4</sup> In an experimental investigation, it was found that the surface coating of Titanium nitride (TiN), Titanium carbide (TiC) on Tungsten carbide cutting tool has given good quality of tribological properties.<sup>5-7</sup> The term high-speed machining refers to end milling at high rotational speeds and high surface feeds. Over the past six decades, High-speed machining (HSM) was used in most of the metallic and non-metallic specimens with the necessity of specific surface topography and the process of materials machining by the hardness of 50HRC and above for the components manufacturing.<sup>8-10</sup> Electrical discharge machining(EDM) with electrodes machining process of particular elements of molds finishing of dimensions like cylindrical, flat and cavity surface through suitable cutting tool materials like cermets, boron nitride etc.<sup>11,12</sup> In an experimental investigation, characteristics of nanostructured coatings for cutting tools were presented and the results revealed that nanostructured coated cutting tools having better wear resistance can make significant serviceable tool properties with specific applications such as high speed and high feed cutting, dry machining etc.<sup>13-15</sup>

Similarly, the design of nano-scale with a procedural approach to multilayered amalgamated coatings was presented and the observed results were compared with standard coatings wear rates.<sup>16-18</sup> Multi ingredients coatings were prepared and the weight of substrate prejudice with various parameters was analyzed and found that the different parameters like hardness, toughness, etc were significantly improved.<sup>19, 20</sup> Cutting tools with the ceramic material are having a property of high-speed processing and normally it won't promise the reliability level of cutting process as needed. In general for developing the process uniqueness of the ceramic material cutting tool a joint treatment should be carried out.<sup>21-23</sup> Wear mechanisms and the reliability of ceramic cutting tools was investigated with and without coatings. From the results, it was observed that the wear rate has been reduced by the necessary coatings. And also found that, the multilayer coatings contents on working surfaces of a tool can provide an improved working reliability and forecast the failures of the cutting tool.<sup>24-28</sup> From the above study, an attempt was made to analyze the mechanical properties of nano material coating of TiN, Titanium aluminum nitride (TiAlN) and titanium aluminum nitride with silicon nitride (TiAlN/Si<sub>3</sub>N<sub>4</sub>) composition cutting tool with required chemical properties.

## EXPERIMENTAL

### Sample preparation

Through physical vapor deposition process, the TiN is coated over the silicon wafer with different coating parameters and nine different samples were obtained with varying mechanical properties. The samples should be parallel to the top and bottom surfaces. The samples are to be free from dirt and adhesive particles that can affect the dimension and the indenting tip. The samples could be cleaned with pressurized air or in an ultrasonic bath.

### Nanoindentation technique

It is an influential procedure used to assess the mechanical properties at nano/microscale and used to find out the different material parameters. Forces concerned are generally in the mille or micro-Newton range and depth of nanometers. A pictorial representation of a nanoindenter is shown in Fig.-1. Nanoindentation method is extensively used for studying the behavior of viscoelastic materials, etc to find the mechanical properties from the load and displacement data.

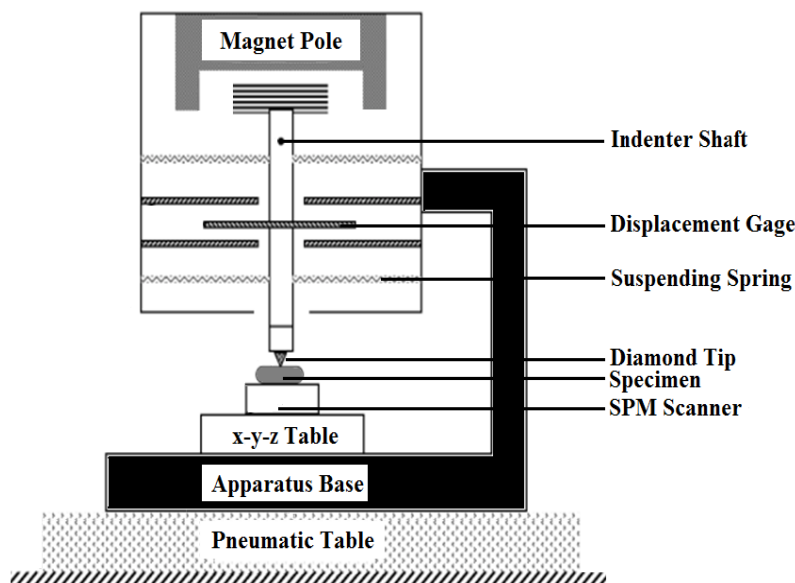


Fig.-1: Working Principle of Nanoindenter

For in-situ studies, the nanoindenters were integrated into transmission electron microscopes to find the correlation among microstructure and deformation. There are numerous review articles related to the nanoindentation were presented in recent studies. Nanoindentation was performed with NT-MTD multi-

mode scanning probing microscope. The indenter used is the Berkovich indenter. The sample size was (1cm x1cm) and the coating thickness of nine samples was between 50-200 nm. Nine samples were loaded under different loading conditions. Each sample was indented 15 times at various locations and the mechanical properties such as hardness (H), Young's modulus (E) and stiffness (S) were obtained. The image of the prepared sample is shown in the following Fig.-2.

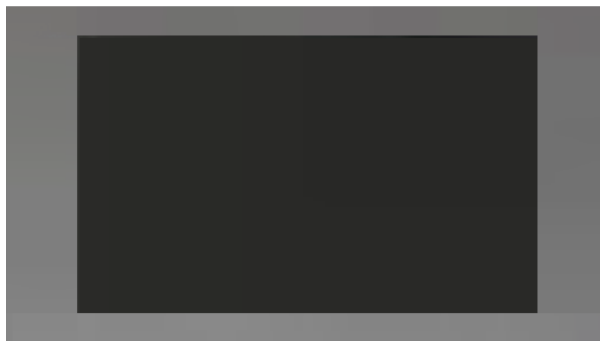


Fig.-2: TiN Sample Image

The sample image before indentation and after indentation of both 2D and 3D were studied by Atomic Force Microscopy (AFM). The AFM 2D and 3D image for the third sample of TiN before and after indentation is given in Fig.-3, Fig.-4, Fig.-5 and Fig.-6 respectively.

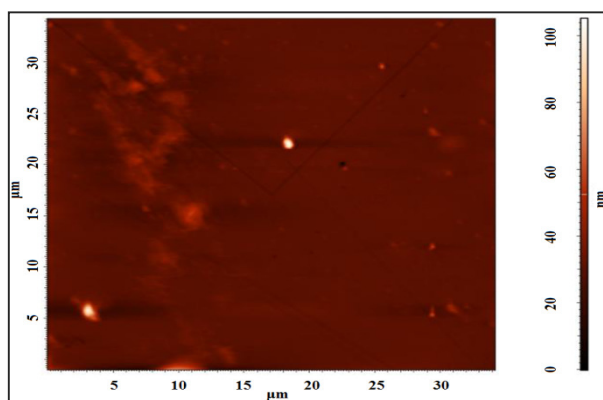


Fig.-3: 2D Image of the Third Sample of TiN before Indentation

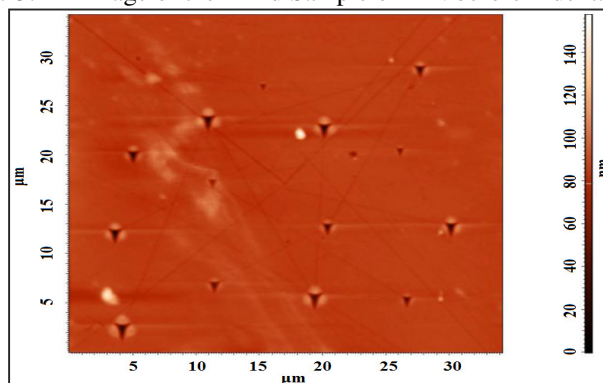


Fig.-4: 2D Image of the Third Sample of TiN after Indentation

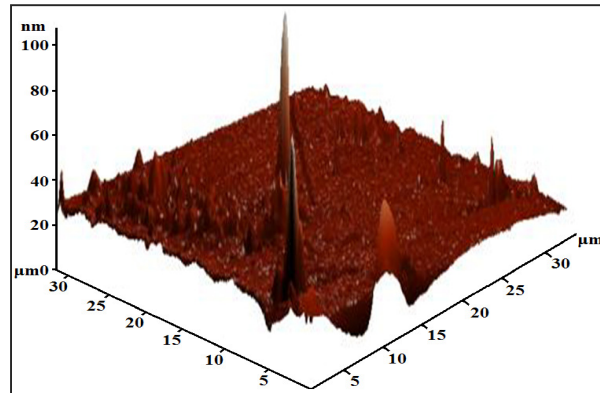


Fig.-5: 3D Image of Third TiN Sample before Indentation

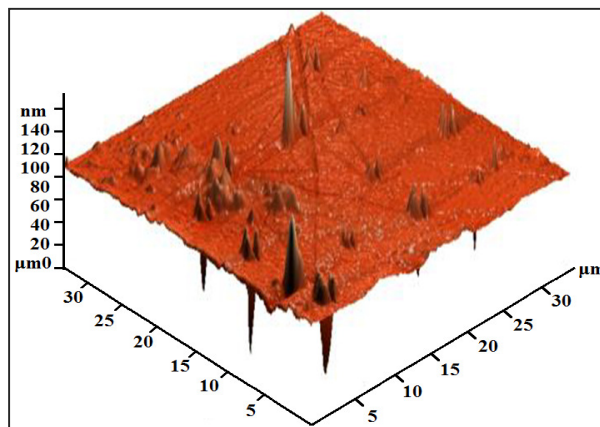


Fig.-6: 3D Image of Third TiN Sample after Indentation

Once the indenter indents the material for a particular loading rate, it could be able to obtain the loading and unloading curve. The load ( $p$ ) Vs displacement ( $h$ ) curve is shown in Fig.-7.

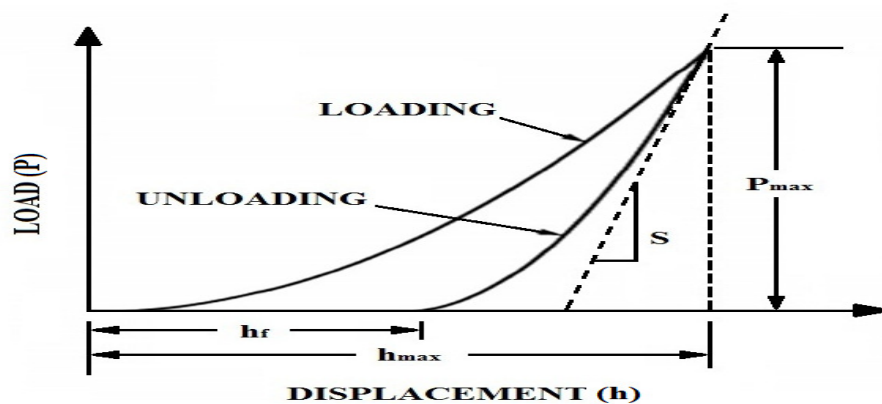


Fig.-7: Pictorial Representation of Load Vs Indenter Displacement Data<sup>29</sup>

Where,

$P_{max}$  = Peak Indentation Load,

$H_{max}$  = Indenter Displacement at Peak Load

$H_f$  = Final Depth of the Contact Impression after Unloading  
 $S$  = Initial Unloading Stiffness.

For particular load, the loading and unloading curve was obtained with the stiffness at the loaded location. The loading and unloading curve for the third sample of TiN is shown in Fig.-8. The red line indicates the loading curve and black indicate the unloading curve.

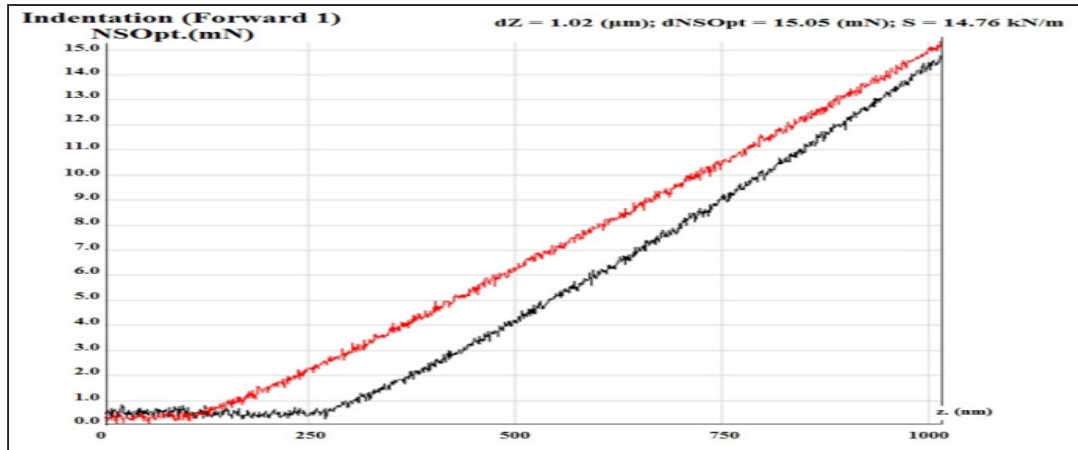


Fig.-8: Loading and Unloading Curve for Third Sample of TiN

**Interpretations of mechanical properties**

Through Oliver-Pharr method the mechanical properties of TiN samples were interpreted which is one of the latest techniques to find out the hardness and modulus of elasticity through sensing indentation of load and displacement. The load-displacement relationships for basic punch geometries can conveniently be written as:

$$P = \alpha h^m \tag{1}$$

Where,

- $P$  = Indenter load
- $H$  = Elastic displacement of the indenter
- $\alpha$  and  $m$  = Constants

Values of exponent 'm' for some of the common punch geometries are  $m = 1$  for flat cylinders,  $m = 2$  for cones,  $m = 1.5$  spheres in the limit of small displacements and  $m = 1.5$  for paraboloids of revolution<sup>30</sup>.

**Reduced modulus**

The reduced modulus was calculated by using the following relation

$$\frac{1}{E_r} = \frac{1 - \nu^2}{E} + \frac{1 - \nu_i^2}{E_i} \tag{2}$$

- Where,  $E$  = Young's modulus for samples
- $\nu$  = Poisson's ratio for samples
- $E_i$  and  $\nu_i$  = Same parameters for the indenter

For TiN sample,  $E = 600\text{Gpa}$ ,  $\nu = 0.25$  for the indenter,  $E_i = 1141\text{Gpa}$  and  $\nu_i = 0.07$

**Stiffness**

The stiffness was found out experimentally or by the following relation knowing all other parameters.

$$\frac{dP}{dh} = 2E * \frac{\sqrt{A}}{\sqrt{P}} \tag{3}$$

Where, P = Load applied  
 H = Maximum indenter displacement  
 $h_c$  = Contact depth  
 $h_s$  = Surface displacement at the contact perimeter

At any time during loading, the total displacement  $h$  is written as:

$$h = h_c + h_s \quad (4)$$

To determine the contact depth the following equation can be used.

$$h_c = h_{\max} - h_s \quad (5)$$

Hardness is defined as the mean pressure where the material will support under load. The hardness is computed from:

$$H = \frac{P_{\max}}{A} \quad (6)$$

## RESULTS AND DISCUSSION

Through the nanoindentation experiment, the maximum depth of indenter travel, hardness, Young's modulus and stiffness were obtained and the values are given in Table-1. From the results, it was found that the maximum hardness of 9.03 was obtained in the sixth sample of TiN with the load of 14.7 mN. Similarly, the average stiffness of all samples falls between 11 and 15 kN/m, except 2nd and 5th sample. The mechanical properties of TiN 6, TiN 7 and TiN 8 were well followed by TiN 3 and TiN 9. The contact depths at the surface, contact area (A), reduced modulus ( $E_r$ ) are interpreted using improved Oliver-Pharr technique and results are given in Table-2. From the results, it was found that the reduced modulus is the maximum in the sample of TiN 7 and minimum in the sample of TiN 5.

Table-1: Nanoindentation Test Results

| Sample | Max. Depth (mm) | Contact Depth (mm) | Load (mN) | Hardness (GPa) | Young's Modulus (GPa) | Stiffness (kN/m) |
|--------|-----------------|--------------------|-----------|----------------|-----------------------|------------------|
| TiN 1  | 660             | 445                | 14.6      | 4.33           | 22.3                  | 11.32            |
| TiN 2  | 400             | 244                | 5.8       | 3.32           | 15.5                  | 7.98             |
| TiN 3  | 362             | 261                | 14.6      | 7.81           | 72.2                  | 14.7             |
| TiN 4  | 660             | 474                | 15.2      | 4.13           | 26.1                  | 12.1             |
| TiN 5  | 717             | 537                | 7.7       | 1.83           | 11.8                  | 4.75             |
| TiN 6  | 394             | 230                | 14.7      | 9.03           | 46.8                  | 14.46            |
| TiN 7  | 337             | 240                | 14.5      | 8.33           | 79.2                  | 15.32            |
| TiN 8  | 351             | 247                | 14.6      | 8.26           | 72.6                  | 14.76            |
| TiN 9  | 422             | 281                | 14.6      | 7.18           | 46.6                  | 14.18            |

Table-2: Interpreted Results using Oliver-Pharr Method

| Samples | Contact Depth at Surface (nm) | Contact Area (nm) <sup>2</sup> | Reduced Modulus ( $E_r$ ) |
|---------|-------------------------------|--------------------------------|---------------------------|
| TiN 1   | 215                           | 0.0034                         | 0.0054                    |
| TiN 2   | 156                           | 0.0017                         | 0.0053                    |
| TiN 3   | 101                           | 0.0018                         | 0.0095                    |
| TiN 4   | 186                           | 0.0036                         | 0.0055                    |
| TiN 5   | 180                           | 0.0042                         | 0.0020                    |
| TiN 6   | 164                           | 0.0016                         | 0.0099                    |
| TiN 7   | 97                            | 0.0017                         | 0.0103                    |
| TiN 8   | 104                           | 0.0017                         | 0.0097                    |
| TiN 9   | 141                           | 0.0020                         | 0.0088                    |

## CONCLUSION

Cutting tools with nanostructured coating can make important functional tool properties with a very good wear resistance for different definite applications. Nine different chemical composition samples with TiN

coated over the silicon wafer by physical vapor deposition process were prepared and the analysis was carried out for each sample. From the observed results, the following conclusions arrived.

- Reduced modulus, contact area, and contact depth were found by obtaining indentation load-displacement data for various peak loads using the Oliver-Pharr technique.
- It was found that, there is a good co-relation between load-displacement data and hardness.
- Samples of TiN 3, TiN 6, TiN 7, TiN 8 and TiN 9 with good chemical composition exhibited good mechanical properties.
- Hence, it could be suggested that the coating on the tungsten carbide cutting tool gives better tool life and better machinability with best chemical composition.
- TiN coating can be considered with suitable levels of output in the machining of aerospace and automobile parts with sufficient practice parameters.
- Further experimental analysis can be carried out for establishing the viability of new coatings through similar constitutive materials with required chemical composition.

### REFERENCES

1. C.M. Kao, Lee, Chen, Chan, Duh and Chen, *Surface and Coatings Technology*, **205**, 1438( 2010)
2. S. Nallusamy, *Journal of Nano Research*, **40**, 99(2016)
3. N. Balasubramanyam, Prasanthi and Yugandhar, *Int. Journal of Adv. Sci. and Tech.*, **75**, 51(2015)
4. S. Nallusamy and A. Manoj Babu, *Journal of Nano Research*, **37**, 58(2015)
5. A. Karthikeyan and S. Nallusamy, *Int. Journal of Engineering Research in Africa*, **31**, 36(2017)
6. S. Nallusamy, *International Journal of Performability Engineering*, **12(2)**, 143(2016)
7. S. Jeevanantham, David Rathnaraj, Robinson Smart, S. Nallusamy and N. Manikanda Prabu, *Indian Journal of Science and Technology*, **9(37)**, 01(2016)
8. S. Sendilvelan, K. Bhaskar and S. Nallusamy, *Rasayan Journal of Chemistry*, **10(2)**, 545(2017)
9. A.S. Vereschaka et al., *Key Engineering Materials*, **581**, 68(2014)
10. S. Nallusamy and A. Karthikeyan, *Indian Journal of Science and Technology*, **9(35)**, 01(2016)
11. Vereshchaka, Sotova, Batako and Vereshchaka, *Journal of Friction Wear*, **35(6)**, 483(2014)
12. S. Nallusamy, *International Journal of Engineering Research in Africa*, **22**, 112(2016)
13. Vereshchaka et al., *Int. Journal of Advanced Manufacturing Technology*, **72(1)**, 303(2014)
14. S. Nallusamy and A. Karthikeyan, *Journal of Nano Research*, **49**, 01(2017)
15. S. Jeevanantham, N.M. Sivaram, D.S. Robinson Smart, S. Nallusamy and N. Manikanda Prabu, *International Journal of Applied Engineering Research*, **12(11)**, 2963(2017)
16. S. Nallusamy, *International Journal of Engineering Research in Africa*, **21**, 110(2015)
17. Vereschaka, Grigoriev and Sladkov, *Applied Mechanics and Materials*, **325-326**, 1454(2013)
18. S. Nallusamy, S. Sendilvelan, K. Bhaskar and N. Manikanda Prabu, *Rasayan Journal of Chemistry*, **10(3)**, 873(2017)
19. C.H. Lai, K.H. Cheng, Lin and Yeh, *Surface and Coatings Technology*, **202(15)**, 3732(2008)
20. S. Nallusamy, *Journal of Nano Research*, **40**, 105(2016)
21. S. Nallusamy and Manikanda Prabu, *International Journal of Nanoscience*, **16(5&6)**, 01(2017)
22. S. N. Grigoriev et al., *Advanced Materials Research*, **1025-1026**, 317(2014)
23. S. Nallusamy, *Pollution Research*, **34(4)**, 721(2015)
24. S. Nallusamy, *Journal of Nano Research*, **45**, 155(2017)
25. S. Nallusamy and Gautam Majumdar, *Int. Journal of Performability Engg.*, **12(3)**, 229(2016)
26. Sergey N. Grigoriev and Alexey A. Krapostin, *Mechanics and Industry*, **17(7)**, 01(2016)
27. S. Nallusamy and J. Logeshwaran, *Rasayan Journal of Chemistry*, **10(3)**, 1050(2017)
28. S. Nallusamy, Manoj Babu and M.K. Prabu, *Int. Journal of Applied Engg. Research*, **10(62)**, 112(2015)
29. M. Stephane, Crecy and V. Mandrillon, *In Proceedings of Int. Con. on Thermal Mechanical and Multi-Physics Simulation and Experiments in Microelectronics and Microsystems*, (2015)
30. T. Schoberl, I.L. Jager and H.C. Lichtenegger, *Applied Scanning Probe Methods*, **13**, 71(2009)

[RJC-1909/2017]